CrystEngComm

Accepted Manuscript

ROYAL SOCIETY OF CHEMISTRY

www.rsc.org/crystengcomm

Journal Name

RSCPublishing

ARTICLE

Intermolecular Anagostic Interactions in Group 10 Metal Dithiocarbamates

Cite this: DOI: 10.1039/x0xx00000x

Ajit N. Gupta,[a] Vinod Kumar,[a] Vikram Singh,[a] Krishna K. Manar,[a] Michael. G. B. Drew[b] and Nanhai Singh*[a]

Received ooth January 2012,
Accepted ooth January 2012

DOI: 10.1039/x0xx00000x

www.rsc.org/

New functionalized homoleptic xanthate and dithiocarbamates of the form $[M(L)_2]$ (M=Ni(II), L = L1 (4-methoxyphenethylxanthate) **1**, L2 (4-ethoxycarbonylpiperadinedithiocarbamate) **2**, L3 (N,N′-difurfuryldithiocarbamate) **3**; M=Pt(II), L3 **4**, M = Pd(II), L4 (N-benzyl-N′-3-methylpyridyldithiocarbamate) **5**) have been synthesized and characterized by microanalyses, and their structures have been investigated by X-ray crystallography. All five complexes are centrosymmetric with the central metal in a distorted square planar structure; the distortion varies in the order Pt >Pd> Ni. In **3**, **4** and **5** the ligand framework and crystal packing effects forces the methylene proton on the substituents in the close proximity of the metal centers forming intermolecular C–H···M (M=Ni, Pt and Pd) anagostic interactions generating 1-D polymeric chain; **4** and **5** are the first examples with Pt and Pd exhibiting such interactions. Similar anagostic interactions are also observed in **2** but are rather weaker. These interactions have been supported by theoretical calculations. The xanthate complex **1** displays unique S···S intermolecular interactions leading to a 1-D polymeric chain, while no significant intermolecular interactions involving the metal centres have been found. The supramolecular structures are sustained by weaker O···H, S···H, C-H···π and C-H···π (chelate, CS_2M) interactions. **1** is weakly conducting, σ_{rt} =1.39x10^{-7} S cm^{-1} but show semiconductor behaviour in the 303-363 K range. The platinum complex **4** shows luminescent property in solution.

Introduction

Much attention has been focused on the metal 1,1-dithiolates owing to their structural diversity, intriguing optical, magnetic and conducting properties, potential applications as sensitizers in solar schemes, single source MOCVD precursors for the preparation of metal sulphides, agriculture, medicine, floatation agents in metallurgy, scavenger for removal of heavy metals from the waste, petroleum additives and as vulcanization accelerators in rubber technology.[1-13] A growing interest in ubiquitous dithiocarbamate and even xanthate ligand complexes is due to the functionalization of substituents on the dithio backbone that may generate a great variety of molecular architectures, afforded by C-H···π, C-H···π (chelate, CS_2M), S···S, S···H and O···H non-covalent and less often through C-H···M agostic, anagostic and hydrogen bonding interactions which modify their chemical reactivity and physical properties.[1-15] The agostic and anagostic interactions are dominated by the organometallic complexes are of broad general interest because of their possible involvement in the organic synthesis through C-H bond activation.[15a,b] In comparison to agostic bonding the nature of anagostic or preagostic interactions has been scantily explored in the literature probably due to the difficulty of assessing whether a ligand forces a hydrogen atom into the vicinity of a transition metal. In recent years intra- and intermolecular anagostic interactions have been demonstrated in a few homo- and heteroleptic dithiocomplexes.[13] Furthermore, the prominent S···S intermolecular stacking contributed significantly in metal 1,2-dithiolates to their higher molecular conductivities.[16]

Notwithstanding some obvious similarities in monoanionic dithiocarbamate and xanthate ligands, they display marked differences in their bonding behaviour and properties due to the choice of variations in functionalities on the nitrogen and oxygen atom of the dithio unit and the dominant resonance structures $\mathbf{R_2N^+{=}CS_2^{2-}}$ and $\mathbf{RO\text{-}CS_2^-}$ that they exhibit in the complexes. Given these facts and in order to gain more insights into anagostic interactions, it was considered worthwhile to undertake the synthesis and structural investigation of some Ni(II), Pd(II) and Pt(II) complexes of functionalized dithiocarbamate and xanthate ligands with a focus on their ability to generate the anagostic interactions in hitherto uninvestigated Pd(II) and Pt(II) dithiocarbamates. The 4-ethoxycarbonylpiperidine, furfuryl, benzyl, 3-methylpyridyl and 4-methoxyphenethyl functionalities on the nitrogen and oxygen atom of the dithiocarbamate and xanthate unit with varying steric bulks have been utilized in order to study their influence on the crystal packing and orientation of the methylene protons to generate M···H-C interactions. The nature of the observed anagostic interactions exhibited by complexes (**3-5**) has been discussed and supported by DFT calculations. The solid phase conductivity of **1** showing efficient S···S intermolecular contacts and the luminescent property of the platinum complex **4** have been studied.

Experimental section

General procedures

All reactions were performed in the open at ambient conditions. Reagent grade chemicals and solvents were procured from commercial sources. The solvents were purified by standard procedures. Potassium salt of the ligands (Scheme 1b), K**L1** (4-methoxyphenylethyl xanthate), K**L2** (4-ethoxycarbonylpiperidine-1-dithiocarbamate), K**L3** (N,N'-difurfuryldithiocarbamate) and K**L4** (N-benzyl-N'-3-methylpyridyldithiocarbamate) were prepared according to literature procedures[12d,e,13b] by the reaction of appropriate alcohol or secondary amines with CS_2 and KOH and characterized by IR, ^{1}H and ^{13}C{^{1}H} NMR spectroscopy. The experimental details pertaining to elemental analysis, recording of IR, ^{1}H and ^{13}C NMR, UV-Vis. absorption and photoluminescent spectra and measurement of pressed pellet electrical conductivity are the same as described elsewhere.[12d,e,13b] The pellet surfaces were coated with the silver paint to make the electrical contact.

Synthesis and characterization of complexes

[M(L)$_2$] (M=Ni(II),L=L1(**1**), L2(**2**), L3(**3**); M=Pt(II), L=L3(**4**); M=Pd(II), L=L4(**5**))

The homoleptic complexes [M(L)$_2$] were synthesized following the general procedure. To a stirring 15 ml solution of the K**L1** (0.266 g, 1 mmol), K**L2** (0.271 g, 1 mmol), K**L3** (0.291 g, 1 mmol) or K**L4** (0.312 g, 1 mmol) in 15 ml MeOH:H_2O (60:40, v/v) was added gradually a 5 ml solution of $NiCl_2.6H_2O$ (0.118 g, 0.5 mmol) or K_2MCl_4 (M=Pd(II), 0.163 g, 0.5 mmol; M=Pt(II), 0.207 g, 0.5 mmol) dissolved in the same solvent mixture at room temperature. The dark green to reddish brown precipitate was formed in a little while. In each case the reaction mixture was stirred for 6 h and the solid product thus formed was filtered off, then washed with methanol followed by diethyl ether. The products so obtained were recrystallized from dichloromethane / methanol mixture, yielding dark green to brown needle shaped crystals of the compounds **1-5**.

[Ni(L1)$_2$] (1). Yield: (0.200 g, 78%), m. p. 161–163^{o}C. Anal. calc. for $C_{20}H_{22}NiO_4S_4$ (533.30): C 46.80, H 4.32%. Found: C 46.58, H 4.35%. IR (KBr, cm^{-1}): ν =1275 (ν_{C-O}), 1042 (ν_{C-S}). ^{1}H NMR (300.40 MHz, $CDCl_3$): δ 7.14 (s, 2H, Ar–H), 6.81 (s, 2H, Ar–H), 4.62 (s, 2H, –CH_2O–), 3.79 (s, 3H, CH_3–OC_6H_4), 3.05 (s, 2H, Ar-CH_2-) ppm. ^{13}C{^{1}H} (75.45 MHz, $CDCl_3$): δ 231.45 (CS_2), 158.88, 128.03, 129.92, 114.35 (Ar–C), 72.70 (CH_3O–), 55..37 (-CH_2-O) 33.74 (Ar-CH_2-) ppm. UV-Vis. (CH_2Cl_2, λ_{max}/nm, Ɛ/M^{-1}cm^{-1}): 255 (4.49 x 10^4), 318 (7.472 x 10^4), 420 (7.72 x 10^3) 651 (1.26 x 10^2). σ_{rt} =1.39 x 10^{-7} S cm^{-1}.

[Ni(L2)$_2$] (2). Yield: (0.211 g, 81%), m. p. 153–155 ^{o}C. Anal. calc. for $C_{18}H_{28}NiO_4N_2S_4$ (523.36): C 41.31, H 5.39, N 5.35%. Found: C 40.92, H 5.34, N 5.22%. IR (KBr, cm^{-1}): ν = 1440 (ν_{C-N}), 1036 (ν_{C-S}). ^{1}H NMR (300.40 MHz, $CDCl_3$): δ 4.20–4.15 (m, 2H, -O-CH_2-Me), 3.26-3.33 (t, 4H, –N(CH_2)$_2$–) , 2.66 (s, 1H, CH-COOEt), 2.03-2.0 (m, 4H, CH(CH_2)$_2$), 1.24-1.29 (t, 3H, CH_3-) ppm. ^{13}C{^{1}H} (75.45 MHz, $CDCl_3$): δ 205.84 (CS_2), 173.17 (-COOEt), 60.83 (-CH_2), 45.51 (N(CH_2)$_2$), 40.22 (C(CH_2)$_2$), 27.31 (CH), 14.15 (CH_3-) ppm. UV-Vis. (CH_2Cl_2, λ_{max}/nm, Ɛ/M^{-1}cm^{-1}): 242 (3.52 x 10^4), 326 (3.29 x 10^4), 400 (6.21 x 10^3) 653 (76).

[Ni(L3)$_2$] (3). Yield: (0.210 g, 78%), m. p. 169–171 ^{o}C. Anal. calc. for $C_{22}H_{20}N_2NiO_2S_4$ (563.35): C 46.91, H 3.58, N 4.97%. Found: C 46.64, H 3.65, N 4.62%. IR (KBr, cm^{-1}): ν =1411 (ν_{C-N}), 1014 (ν_{C-S}). ^{1}H NMR (300.40 MHz, $CDCl_3$): δ 7.40 (s, 1H) 6.37-6.36 (m, 2H), 4.75 (s, 2H) ppm. ^{13}C {^{1}H}NMR (75.45 MHz, $CDCl_3$) δ 209.71 (CS_2), 147.41, 143.11, 110.65 (C_4H_3O), 44.17 (–CH_2–C_4H_3O) ppm. UV-Vis. (CH_2Cl_2, λ_{max}/nm, Ɛ/M^{-1}cm^{-1}): 250 (4.15 x 10^4), 327 (4.59 x 10^4), 400 (8.88 x 10^3) 640 (45).

[Pt(L3)$_2$] (4). Yield: (0.244 g, 70%), m. p. 194–196 ^{o}C. Anal. calc. for $C_{22}H_{20}N_2PtO_2S_4$ (699.73): C 37.26, H 2.88, N 4.00%. Found: C 36.85, H 2.95, N 3.65%. IR (KBr, cm^{-1}): ν =1412 (ν_{C-N}), 1013 (ν_{C-S}). ^{1}H NMR (300.40 MHz, $CDCl_3$): δ 7.40 (s, 1H) 6.40-6.36 (m, 2H), 4.75 (s, 4H) ppm. ^{13}C {^{1}H}NMR (75.45 MHz, $CDCl_3$) δ 204.25 (CS_2), 147.17, 143.21, 110.84 (C_4H_3O), 44.25 (–CH_2–C_4H_3O) ppm.. UV-Vis. (CH_2Cl_2, λ_{max}/nm, Ɛ/M^{-1}cm^{-1}): 255 (1.36 x 10^5), 292 (4.28 x 10^4), 352 (7.1 x 10^4), 411 (8.34 x 10^3).

[Pd(L4)$_2$] (5). Yield: (0.244 g, 75%), m. p. 245–247 ^{o}C. Anal. Calc. for $C_{28}H_{26}PdN_4S_4$ (653.20): C 51.49, H 4.01, N 8.58%. Found: C 51.15, H 3.98, N 8.32%. IR (KBr, cm^{-1}): ν =1453 (ν_{C-N}), 1028 (ν_{C-S}). ^{1}H NMR (300.40 MHz, $CDCl_3$): δ 8.48-8.59 (d, 2H py) 7.29-7.71 (m, 7H), 4.82 (s, 4H, -$CH_2C_5H_4N$, -$CH_2C_6H_5$) ppm. ^{13}C {^{1}H}NMR (75.45 MHz, $CDCl_3$) δ 213.64 (CS_2), 149.65, 136.12, 133.38, 129.85, 128.90, 123.90 (C_6H_5-, C_5H_5N), 51.30 (–CH_2–C_5H_5N) 48.49 (-$CH_2C_6H_5$) ppm. UV-Vis. (CH_2Cl_2, λ_{max}/nm, Ɛ/M^{-1}cm^{-1}): 240 (3.96 x 10^4), 307 (1.28 x 10^5), 356 (1.0 x 10^4).

Crystallography

Single crystal X-ray data for **1-5** were collected on Oxford Diffraction X-calibur CCD diffractometers at 150 K for **1**,**3** and **4** and at 293 K for **2** and **5**, using Mo Kα radiation. Data reduction was carried out using the CrysAlis program.[19] The structures were solved by direct methods using SHELXS-97[20] and refined on F^2 by full matrix least squares technique using SHELXL-97.[20] In **5**, the nitrogen in the pyridine ring is disordered over two sites. Non-hydrogen atoms were refined anisotropically and hydrogen atoms were geometrically fixed with thermal parameters equivalent to 1.2 times that of the atom to which they were bonded. Diagrams for all complexes were prepared using ORTEP, Mercury and Diamond softwares.[21] The .cif files have been deposited at the Cambridge Crystallographic Data Centre with reference numbers CCDC No. 997873-997877for **1-5** respectively.

Theoretical Calculations

All calculations were carried out using the Gaussian 03 program.[22] Calculations were carried out using the B3LYP density functional together with basis sets LANL2DZ for Ni, Pd and Pt, 6-31+G* for S and 6-31G for the remaining atoms. Starting models were taken from the crystal structures but with hydrogen atoms given theoretical positions.

Results and Discussion

Synthesis and spectroscopy

Complexes **1-5** were isolated in good yield (Scheme 1) by treating one equivalent of the metal salt solution with two equivalents of the potassium salt of ligands, K**L1**-K**L4** (Scheme 1a) in MeOH:H_2O mixture. All the complexes are air and moisture stable, melt in the 153-247^{o}C temperature range. These complexes have been characterized by elemental analysis, IR, NMR and UV-Vis. spectroscopy. The electrical conductivity of **1** and photoluminescent property of **4** have been studied. The structures of **2-5** revealed rare M···H-C (M= Ni, Pt, Pd) intermolecular anagostic interactions which have been corroborated by theoretical calculations.

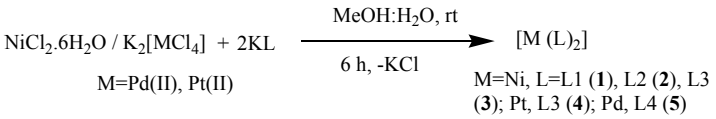

Scheme 1a. General methodology for the synthesis of complexes **1-5**.

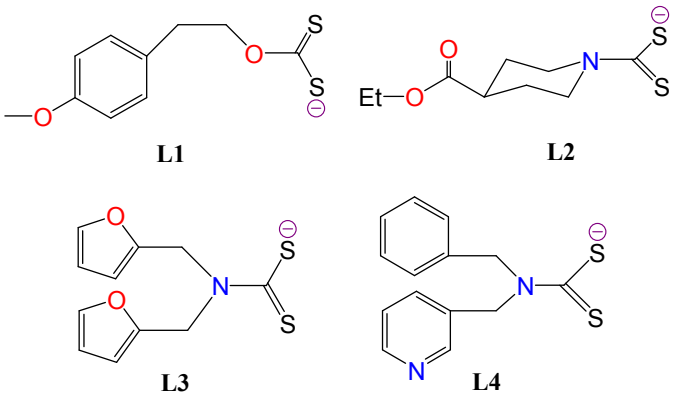

Sceme 1b. Structure of the ligands (**L1-L4**) used in this work.

IR spectra of **1-5** show bands at 1275, 1013-1042 and 1411-1453 cm^{-1} diagnostic of the $\nu_{(C-O)}$, $\nu_{(C-S)}$ and $\nu_{(C-N)}$ frequencies for the coordinated xanthate and dithiocarbamate ligands. A noticeable enhancement of 126-155 cm^{-1} in the $\nu_{(C-N)}$ vibrations in the dithiocarbamate complexes in comparison to free ligands show partial double bond character of the C-N bond due to significant contribution of the resonance form $\mathbf{R_2N^+{=}CS_2^{2-}}$. (*vide infra in the crystal structures*).

In the ^{1}H NMR spectra, **1-5** show sharp resonances associated with the ligand functionalities and are consistent with the composition of complexes. The expected downfield shift in the ^{1}H NMR for the methylene proton of the ligands at room temperature in **3-5** involved in the intermolecular C-H···M (Ni, Pt, Pd) anagostic interactions as revealed by X-ray structural determinations (*vide infra*) was not observed and therefore the existence of these interactions in solution could not be confirmed. However in the low temperature NMR spectra of **5** in $CDCl_3$, the methylene proton observed as a singlet at δ 4.820 ppm at 25^{o}C begins to broaden at -25^{o}C and at -40^{o}C separated into two singlets at δ 4.778 and 4.789 ppm thereby indicating the involvement of the methylene proton H(31A) in anagostic interactions with the metal center (Fig. 1). In the case of **3** and **4** no such splitting was observed at lower temperature. In the ^{13}C NMR spectra, a single low field signal at δ 231 ppm in **1** and at δ 205-213 ppm in (**2-5**) are characteristic of the OCS_2 and NCS_2 carbons of the xanthate and dithiocarbamate ligands respectively. Notably because of the dominant contribution of resonance form $\mathbf{R_2N^+{=}CS_2^{2-}}$in the dithiocarbamate complexes, the NCS_2 carbon is more shielded than the free ligands hence the ^{13}C signal is moved to higher field in the complexes than the free ligands (δ =212.21-216.65 ppm). Conversely in **1** the

OCS_2 ligand carbon shows a perceptible downfield shift as compared to that found in the free xanthate because of the significant contribution of resonance form **RO-CS_2^-** in this complex.

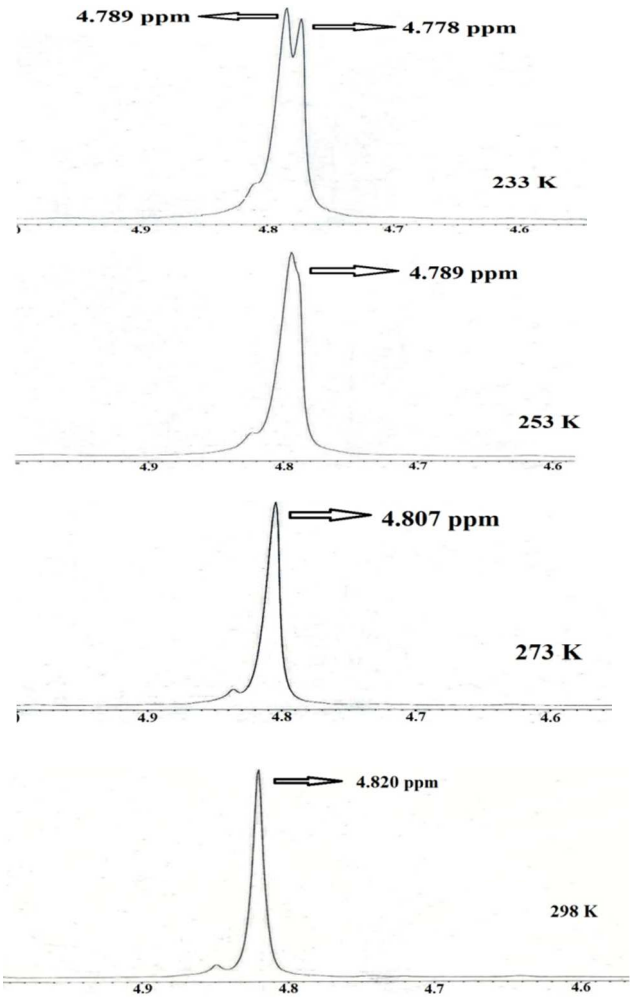

Fig. 1 Partial ^{1}H NMR spectra of **5** at variable temperature.

The electronic absorption spectra of **1-5** (Fig. 2) in the dichloromethane display medium to strong bands near 240-350 nm (Ɛ=32,900-1,36,000$M^{-1}cm^{-1}$) and 360-420 nm (Ɛ=6200-10,000$M^{-1}cm^{-1}$) which are assignable to intraligand charge transfer (ILCT) and ligand to metal charge transfer (M←S, LMCT) transitions respectively; additionally, for the nickel complexes **1-3** a weak broad absorption band observed near 650 nm (Ɛ=45-126 $M^{-1}cm^{-1}$) is assigned to d-d transition consistent with a square planar geometry[17] about the metal center in these complexes.

Upon excitation at 350 nm the platinum complex **4** exhibits a broad unstructured emission band at 450 nm (Fig. 2) which emanates from the LMCT state. The nickel and palladium complexes do not show luminescent behaviour.

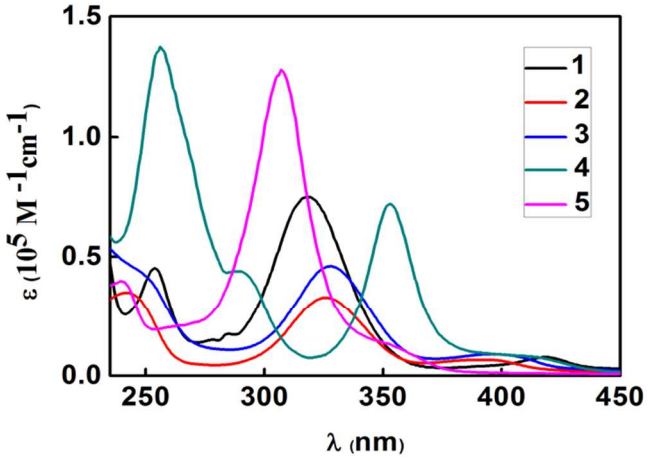

a

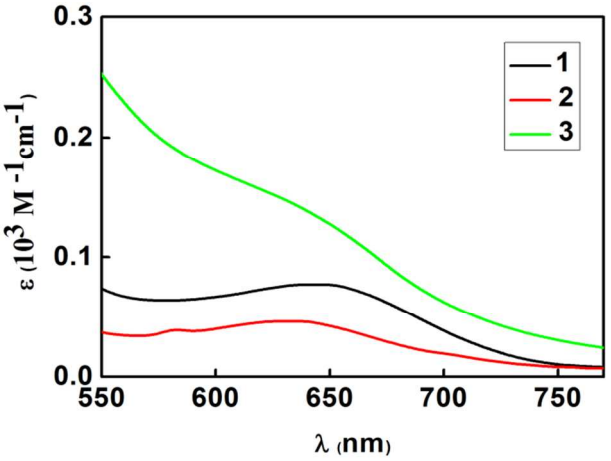

b

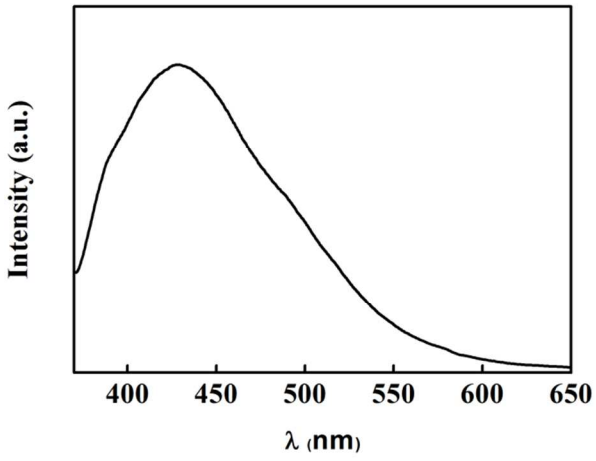

c

Fig. 2 (a) UV–Vis. absorption spectra in CH_2Cl_2 showing intraligand and ligand to metal charge transfer for **1–5,** (b) d–d transitions for **1-3** and (c) Photoluminescent spectra of **4.**

Crystal Structures

Single crystals of **1**, **3**, **4** and **5** were grown by slow evaporation of the dichloromethane solution of the compounds while that of **2** by layering of methanol in the same solvent. Selected bond distances, bond angles and crystallographic details are listed in Tables 1 and S1, ESI and ORTEP diagrams for **1-5** are shown in Fig. 3. Structures **3** and **4** are isomorphous.

In all five complexes the metal atom lies on an inversion centre, thus each asymmetric unit contains half a discrete molecule. The geometry about the metal centres is four coordinate distorted square planar. While the equatorial MS_4 moiety is perforce planar, distortion arises because of the small bite angle S(11)-M-S(13) which falls in the range 79.43(3)-79.51(3)^o for **1-3** and 74.75(6)^o for **4** and 75.64(10)^o for **5** . There is little difference between M-S bond lengths in each structure being in the range 2.195(1)-2.216(1) Å for **1-3** (M=Ni), while Pt-S bonds in **4** are 2.319(2), 2.320(2) Å, slightly shorter than the Pd-S bonds in **5** at 2.340(3), 2.335(3) Å. The four membered MS_2C rings in the five structures show no significant deviations from planarity.

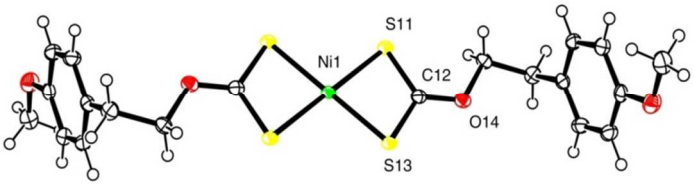

1

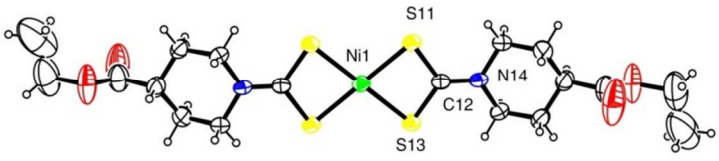

2

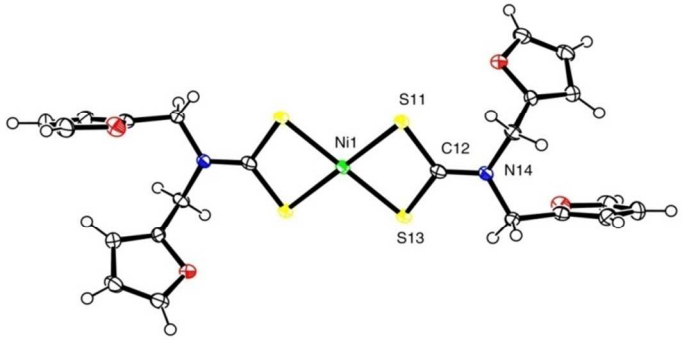

3

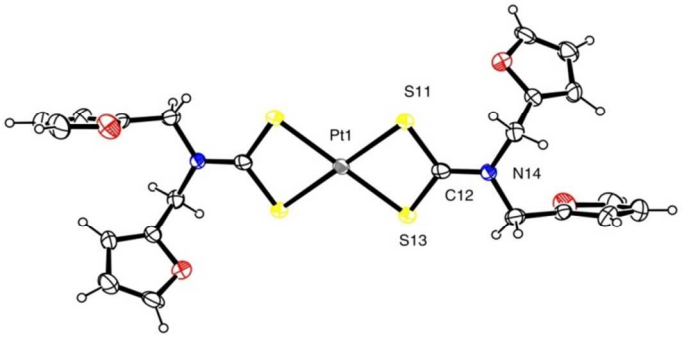

4

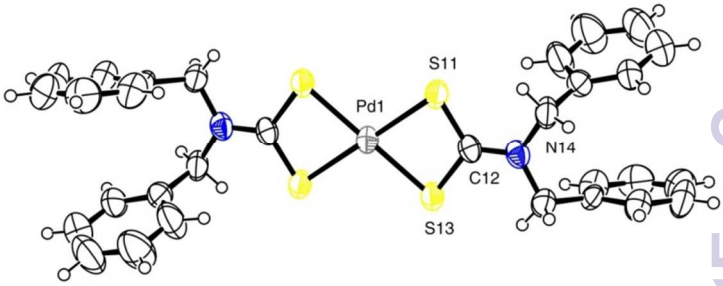

5

Fig. 3 ORTEP diagrams for **1-5** with ellipsoids drawn at the 50% probability level for **1**, **3** and 30% for **2, 4** and **5**. All five structures contain crystallographic centres of symmetry. **3** and **4** are isomorphous.

Table 1. Selected bond lengths (Å) and bond angles (°) for **1-5**.

	1 (X=O, M=Ni)	**2** (X=N, M=Ni)	**3** (X=N, M=Ni)	**4** (X=N, M=Pt)	**5** (X=N, M=Pd
M(1)–S(11)	2.2072(8)	2.2071(12)	2.2016(9)	2.3188(17)	2.340(3)
M(1)–S(13)	2.2161(8)	2.1893(12)	2.1951(9)	2.3195(17)	2.335(3)
S(11)–C(12)	1.693(3)	1.727(4)	1.722(3)	1.734(6)	1.713(8)
S(13)–C(12)	1.696(3)	1.718(4)	1.727(3)	1.706(7)	1.757(8)
C(12)–X(14)	1.305(3)	1.297(6)	1.313(4)	1.326(7)	1.310(9)
S(11)–M(1)–S(13)	79.43(3)	79.47(4)	79.51(3)	74.75(6)	75.64(10)
M(1)–S(11)–C(12)	83.94(10)	85.11(15)	85.57(12)	87.4(2)	86.8(3)
M(1)–S(13)–C(12)	83.60(11)	85.88(15)	85.66(12)	88.0(2)	86.0(3)
S(11)–C(12)–S(13)	113.02(17)	109.3(3)	109.25(19)	109.9(4)	111.4(4)

In **1** because of the appropriate orientation of the substituent on the oxygen atom of the xanthate ligand, the closest S(11)···S(11) (-1-x, -1-y, -z) intermolecular distance of 3.461(2) Å, between the coordinated ligands is less than the sum of the vander Waals radii of sulphur (3.60 Å) thus demonstrating S···S intermolecular interactions constructing a 1-D polymeric chain motif (Fig. 4). The supramolecular structure is sustained through the intermolecular methylene C(15)-H···π(chelate, CS_2Ni)distances of 2.61 Å and C-H···π interactions between H(28C) (a methyl proton), centroid of the phenyl ring and H(16B) (a methylene proton), centroid with distances 2.79 and 3.27 Å (Fig. 4) respectively. A similar C-H···Ni anagostic interaction with Ni···H distance of 2.908 Å and ∠C-H···Ni 149° is also observed in **2** but is somewhat weaker. (Fig. S1, ESI).

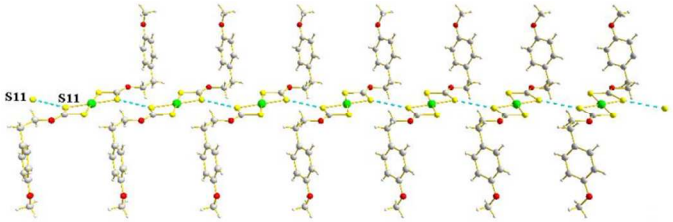

a

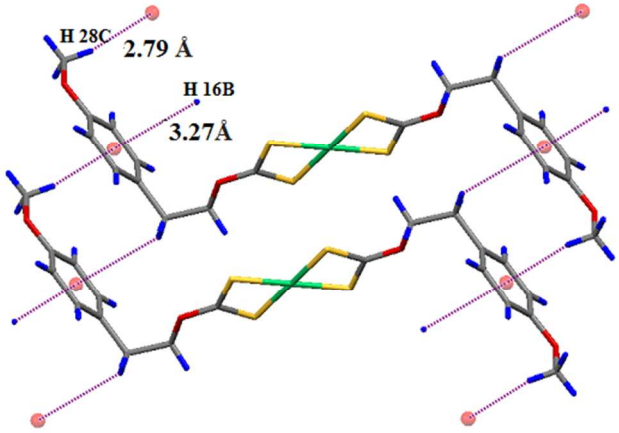

b

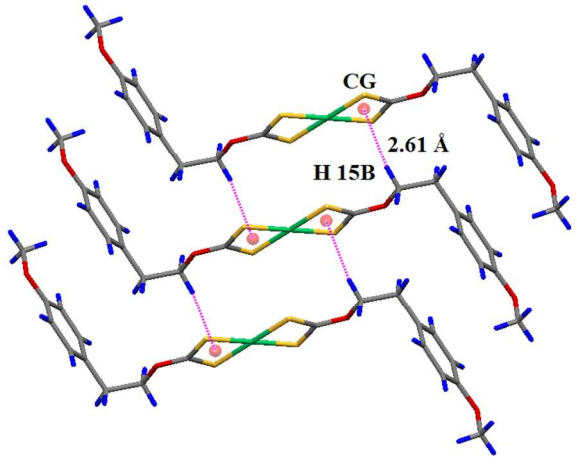

c

Fig. 4 The structure of **1** (a) 1D-polymeric chain motif network through unique S···S interactions, (b) C-H···π interactions and (c) C-H···π(chelate, CS_2Ni) interactions.

The most characteristic feature of **3** and **4,** which are isomorphous, and **5** is that the ligand framework and crystal packing effects forces the C-H proton of methylene groups on the ligand substituents in the close proximity of the metal centers forming significant intermolecular C-H···M (Ni, Pd, Pt) anagostic or preagostic interactions generating 1-D polymeric chain motifs; in these structures the vacant axial sites on the metal centres are occupied by C-H protons providing pseudo octahedral coordination environment. The C-H···M distances of 2.61, 2.80 and 2.79 Å and ∠C-H···M angles of 148, 147 and 154° in **3-5** respectively are well within the range of anagostic interactions.[13] These metric data indicate attenuation in the anagostic interactions from Ni >Pd>Pt. Though reported in a few analogous nickel dithiocarbamates, and xanthate complexes,[13b,c] the platinum **4** and palladium **5** dithiocarbamates are the first examples depicting such type of interactions. It is to be noted that the agostic bond is a 3c-2e type formed with electron deficient early transition metals and accompanied with an upfield shift compared to uncoordinated C-H protons whereas the anagostic or preagostic interactions

which are largely electrostatic in nature and are typically associated with the metal, d^8 or even d^9 square planar complexes showing a downfield shift of C-H protons. A good account of these characteristic features are provided in the literature.[15] The metric parameters for such two types of interactions are distinctly different as the M-H distances range from 1.8-2.3 Å and 2.3–2.9 Å and the ∠C-H···M from 90-140° and 110-170° for the agostic and anagostic bondings respectively, the latter being more electrostatic in character. A third type of bond, namely 3c-4e consisting of a nearly linear M···H-X (X=F,O,N,C) interaction is known and recognised by a considerable downfield shift of the participating proton. X-ray crystal structures and ^{1}H NMR spectroscopy are crucial for elucidation of these interactions but despite advance quantum chemical calculations their origin is still a matter of debate. A detailed analysis of the position of the anagostic methylene hydrogen atom in **3**, **4** and **5** shows some interesting features. In particular it would appear that the hydrogen atom in **3** and **4** is directed more towards the centre of gravity (CG) of the chelate ring than the metal atom. Thus M-H distances are 2.61, 2.80 Å while CG···H distances are 2.61, 2.74 Å respectively. In addition C-H···M and C-H···CG angles are 148, 172° in **3** and 147, 169° in **4**. By contrast in **5**, the hydrogen is closer to the metal with distance 2.79 Å, angle 154° than with the CG 3.23 Å, 129°.The interactions with the hydrogen weakened in the order Ni > Pt >Pd presumably due to variations in the size of the metal and the steric bulk of the substituents on the dithiocarbamate unit.

Calculations were carried out to investigate these differences in the relative hydrogen position for **3**, **4** and **5**. Two models were created, a monomer and then a trimer consisting of a central molecule with two additional molecules with the hydrogen atoms in axial positions as shown in Figure 4c. Single point calculations were carried out and showed that the energy difference, E(trimer)-3*E(monomer) were -13.84, -8.24, -16.03 kcalmol^{-1} for **3**, **4** and **5** respectively, thus showing that the interaction of the hydrogen with the metal in **5** is stronger than that with the MS_2C ring in **3** and **4**.

The models for structures **3** and **5** were then geometry optimised. The energy differences E(trimer)-3*E(monomer) increased to -23.29, -21.39 kcalmol^{-1}. In particular we investigated the positions of the H atoms relative to the metal and the CG of the four-membered ring. In **3**, the H atom became approximately equidistant from Ni at 2.75Å and CG at 2.74Å although it was directed more towards the CG (C-H···CG 177°) than the metal (C-H···Ni 149°). By contrast in **5** the H atom remained in an axial position although the Pd-H distance increased in 3.13Å. In both optimisations distances involving the H with M and/or CG increased which suggests that the interactions are held together to some extent by molecular packing and not entirely by intramolecular electronic effects.

In **3** and **4** the five-membered rings on the dithiocarbamate ligands are less parallel to the six-membered rings as compared to that of the palladium complex **5**. Thus the orientation of the methylene proton is slightly changed and comes closer to the chelate CG. The angles CG-M-H in **5** are closer to perpendicular at 90° than the 73, 75° observed in **3** and **4** (Table 2) thereby indicating smaller distortion in the pseudo octahedral geometry (Fig. 5) which may be the result of 5+5 (**3,4**) and 6+6 (**5**) ring systems; this distortion brings the methylene hydrogen closer to the MS_2C chelate ring CG in **3** and **4** than in **5**.

Table 2. Important geometric parameters for the anagostic interactions in **3-5**.

Complex	M···H/Å	∠C–H···M/°	CG···H/Å	∠C-H···CG/°	∠H-M-CG/°
3	2.61	148	2.61	172	73
4	2.80	147	2.74	169	75
5	2.79	154	3.23	129	90

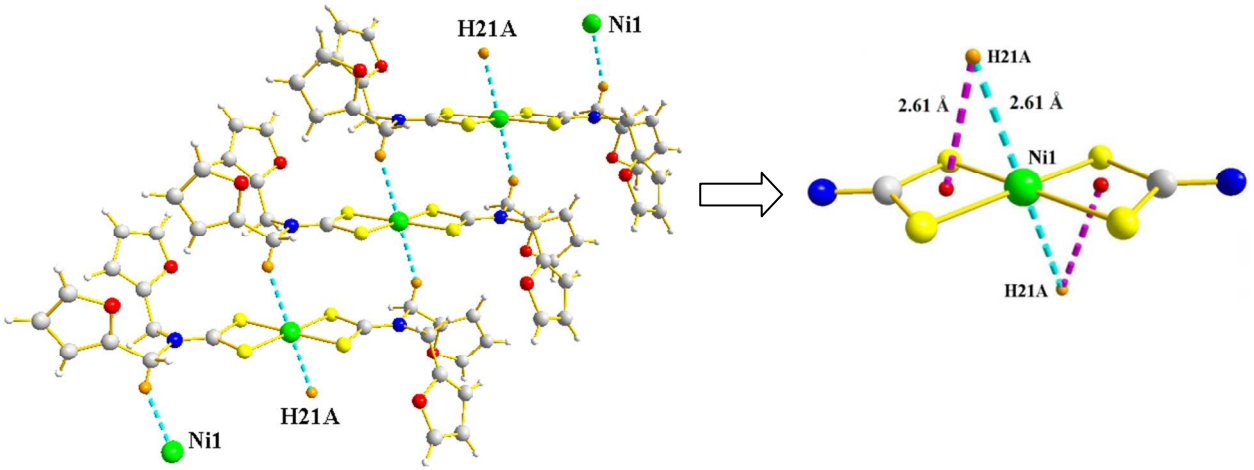

3

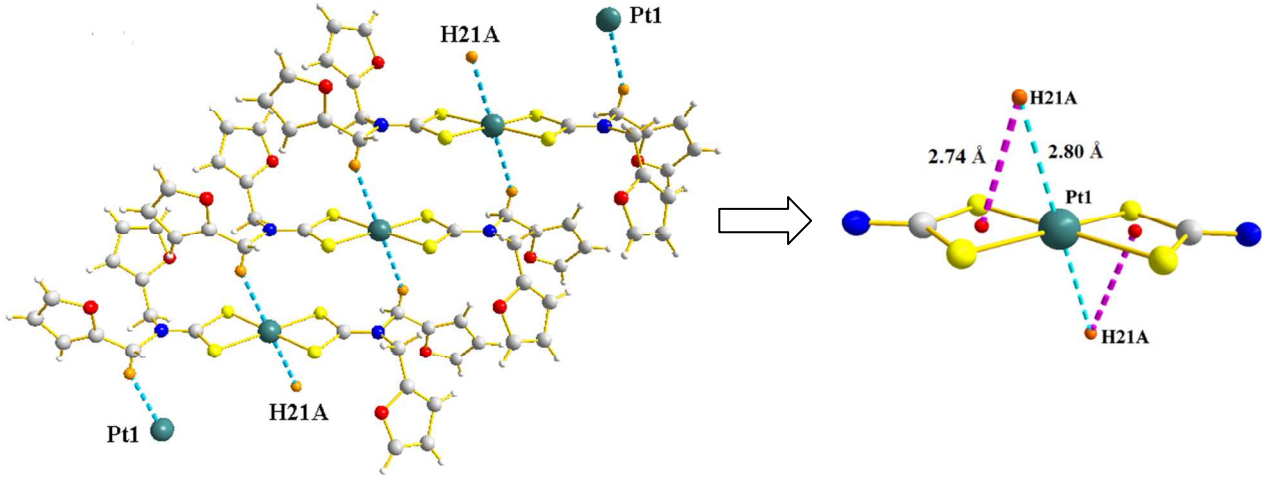

4

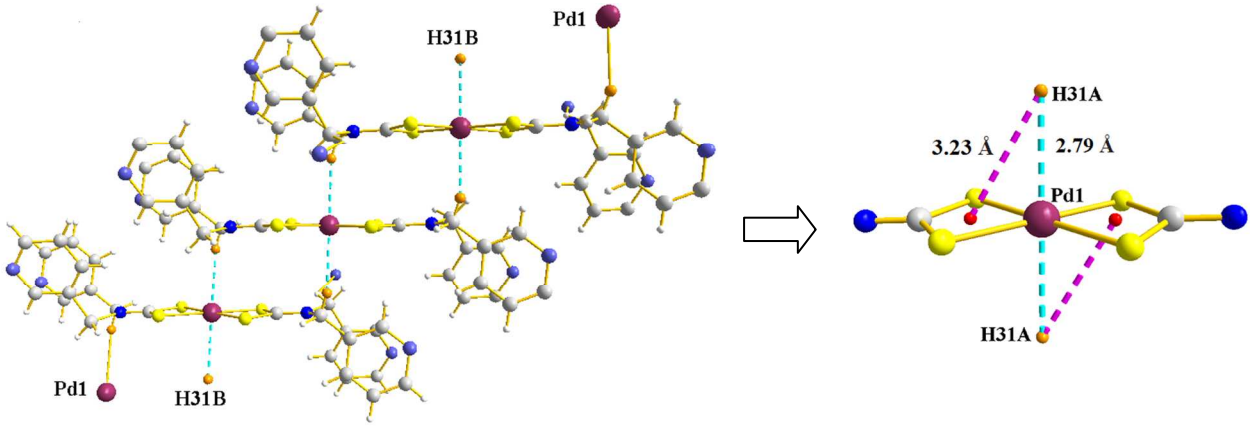

5

Fig. 5 Intermolecular M···H-C anagostic and CG···H-C interactions in **3-5** presenting 1-D polymeric chain motifs along with their core. Colour code: Ni, Bright green; Pd, Plum; Pt, Teal; S, Yellow; N, Ink blue; C, Grey; O, Red; H, Light orange.

The closest S···S intermolecular distances between the coordinated dithiocarbamate ligands in **3-5** fall in the 3.925-4.225 Å range and are significantly larger than that observed in the xanthate complex **1,** a fact which indicates the absence of effective S···S intermolecular association in these complexes. In all the complexes the supramolecular architectures are stabilized via weaker S···H and O···H noncovalent interactions (Fig. S2, ESI). The C(12)–O(14) and C(12)–N(14) distances of 1.304(4) Å in **1** and in the range of 1.297(6)-1.326(7) Å **2-5** are concomitant with the resonance structures.[1,2] The C-S bond lengths of 1.694(3) and 1.698(3) Å in the xanthate complex **1** are slightly smaller than those of 1.706(7)-1.757(8) Å in the dithiocarbamate complexes **2-5,** though all are significantly shorter than the C-S single bond (ca.1.81Å) due to π delocalization over the NCS_2 units.

Electrical conductivity

The molecular electrical conductivity of the xanthate complex **1** has been measured using the complex impedance spectroscopy in the 303-363K temperature range at 100 kHz frequency with powdered sample as pressed pellet sandwiched by silver electrodes (diameter: 13.2 mm; the pellet thickness of 0.95 mm. It is now well established that the extent of S···S intermolecular stacking in the extended π delocalised structures plays a key role for higher conductivities of the metal dithiolates.[16] The σ_{rt} value of 1.39×10^{-7} S cm^{-1} shows its weakly conducting behaviour. It is worth mentioning that despite efficient S···S intermolecular contacts of 3.461(2) Å (*vide supra in the crystal structure*), the conductivity of **1** is much smaller which may be attributed to the less conjugated extended molecular array in comparison to metal 1,2-dithiolates.[16] Its σ value is correlated with temperature (Fig. 6) thus showing semiconductor properties. The remaining complexes are even more weakly conducting due to abscence of intermolecular S···S stacking unlike **1**.

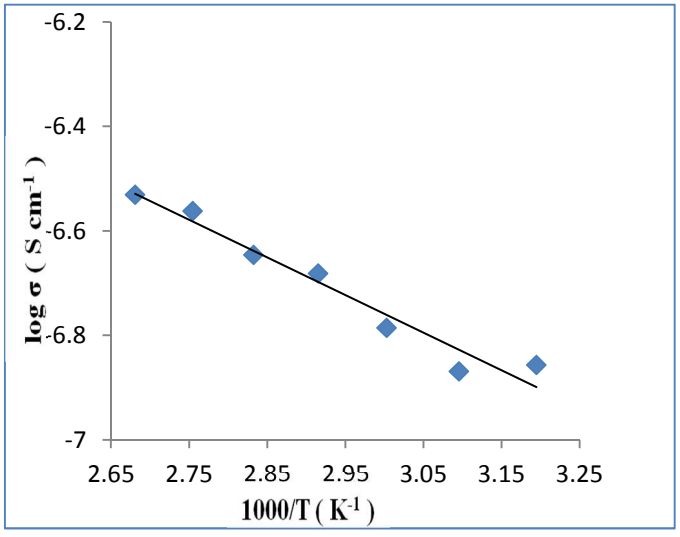

Fig. 6 Temperature dependant solid phase conductivity of **1**.

Conclusions

New Ni(II), Pd(II) and Pt(II) homoleptic dithiocarbamates **2-5** and xanthate **1** have attractive structural features delineating unique intermolecular C-H···M anagostic and S···S interactions respectively generating 1-D polymeric chains. These anagostic interactions are weakened Ni>Pd>Pt. **4** and **5** are the first examples of the platinum and palladium dithiocarbamates displaying intermolecular anagostic interactions. **1** is weakly conducting but showed semiconductor behaviour in the solid phase. The anagostic interactions are of significant importance from the view point of crystal engineering and their possible role in catalysis for C-H bond activation. This study widens the scope for underexplored functionalized dithio ligand complexes that may display anagostic and S···S intermolecular interactions for their possible applications as novel functional materials.

Acknowledgements

The Council of Scientific and Industrial Research (CSIR), Project No. 01(2679)/12/EMR-II (NS), University Grants Commission (ANG) SRF, New Delhi and the Department of Chemistry, Banaras Hindu University, Varanasi INDIA for the Oxford diffraction X-calibur CCD diffractometer, which was used for structures **2** and **5**, are gratefully acknowledged. The EPSRC and the University of Reading are thanked for funds for the Oxford diffraction X-calibur CCD diffractometer used for structures **1**, **3** and **4**.

Notes and references

[a]Department of Chemistry, Banaras Hindu University, Varanasi 221005, India.
[b]Department of Chemistry, University of Reading, Whiteknights, Reading, RG6 6AD, U.K.

† Footnotes should appear here. These might include comments relevant to but not central to the matter under discussion, limited experimental and spectral data, and crystallographic data.

Electronic Supplementary Information (ESI) available: [details of any supplementary information available should be included here]. See DOI: 10.1039/b000000x/

1(a) D. Coucouvanis, *Prog. Inorg. Chem.*, 1970, **11**, 233; (b) D. Coucouvanis, *Prog. Inorg. Chem.*, 1979, **26**, 301.

2. G. Hogarth, *Prog. Inorg. Chem.*, 2005, **53**, 71.

3. P. J. Heard, *Prog. Inorg. Chem.,* 2005, **53**, 268.

4. (a) E. R. T. Tiekink and I. Haiduc, *Prog. Inorg. Chem*., 2005, **54**, 127; (b) C. S. Lai and E. R. T. Tiekink, *CrystEngComm*, 2003, **5**, 253.

5 J. Cookson and P. D. Beer, *Dalton Trans.*, 2007, **15**, 1459.

6. E. J. Mensforth, M. R. Hill, S. R. Batten, *Inorg. Chim. Acta*, 2013, **403**, 9.

7. (a) S. Naeem, S. A. Serapian, A. Toscani, A. J. P. White, G. Hogarth and J. D. E. T. Wilton-Ely, *Inorg. Chem.* 2014, **53**, 2404; (b) O.D. Fox, M. G. B. Drew, P. D. Beer, *Angew. Chem., Int. Ed. Engl.* 2000, **39,** 135; (c) M.E. Padilla-Tosta, O. D. Fox, M. G. B. Drew, P. D. Beer, *Angew. Chem., Int. Ed. Engl.* 2001, **40** , 4235.

8. (a) T. Okubo, N. Tanaka, K. H. Kim, H. Yone, M. Maekawa and T. Kuroda-Sowa, *Inorg. Chem*., 2010, **49**, 3700; (b) T. Okubo, H. Anma, N. Tanaka, K. Himoto, S. Seki, A. Saeki, M. Maekawa and T. Kuroda-Sowa, *Chem. Commun*., 2013, **49**, 4316.

9. (a) P, O' Brien and J. H. Park, J. Waters, *Thin. Solid. Films*, 2003, **431**, 502; (b) N. Alam, M. S. Hill, G. Kociok-Kohn, M. Zeller, M. Mazhar and K. C. Molloy, *Chem. Mater.*, 2008, 20, 6157; (c) Y. S. Tan, A. L. Sudlow, K. C. Molloy, Y. Morishima, K. Fujisawa, W. J. Jackson, W. Henderson, S. N. B. A. Halim, S. W. Ng and E. R.T. Tiekink, *Cryst. Growth Des*. 2013, **13,** 3046.

10 A. A. Abramov, K. S. E. Forssberg, *Miner. Process. Extr. Metall. Rev.* 2005, **26**, 77.

11.(a) R. F. Semeniuc, T. J. Reamer, J. P. Blitz, K. A. Wheeler, and M. D. Smith *Inorg. Chem.* 2010, **49**, 2624; (b) Y. Yan, S. Krishnakumar, H. Yu, S. Ramishetti, L.-W. Deng, S. Wang, L. Huang, and D. Huang, *J. Am. Chem. Soc.* 2013, **135**, 5312.

12. (a) A. Kumar, R. Chauhan, K. C. Molloy, G. Kociok-Kohn, L. Bahadur and N. Singh, *Chem. Eur. J.*, 2010, **16**, 4307; (b) V. Singh, R. Chauhan, A. N. Gupta, V. Kumar, M. G. B. Drew, L. Bahadur and N. Singh; (c) S. K. Singh, R. Chauhan, B. Singh, K. Diwan, G. Kociok Kohn, L. Bahadur and N. Singh, *Dalton Trans.*, 2012, **41**, 1373; (d) V Singh, A. Kumar, R. Prashad, G. Rajput and N. Singh, *CrystEngComm*, 2011, **13**, 6817. (e) A. N. Gupta, V. Singh, V. Kumar, A. Rajput, L. Singh, M. G. B. Drew and N. Singh, *Inorg. Chim. Acta*, 2013, **408**, 145.

13. (a) R. Angamuthu, L. L. Gelauff, M. A. Siegler, A. L. Spek and E. Bouwman, *Chem. Commun*., 2009, 2700; (b) G. Rajput, V. Singh, A. N. Gupta, M. K. Yadav, V. Kumar, S. K. Singh, A. Prashad, M. G. B. Drew and N. Singh, *CrystEngComm*, 2013, **15**, 4676. (c) S. K. Singh, M. G. B. Drew and N. Singh *CrystEngComm,* 2013, **15**, 10255; (d) B. Singh, M. G. B. Drew, G. K.-Kohn, K. C. Molloy and N. Singh, *Dalton Trans.*, 2011, **40**, 623; (e) S. K. Singh, K. Diwan, M. G. B. Drew and N. Singh, *Inorg. Chim. Acta*, 2012, **384**, 176.

14. G. R. Desiraju, *Chem. Commun*., 2005, 2995.

15 (a) M. Brookhart, M. L. H. Green and G. Parkin, *Proc. Natl. Acad. Sci. U. S. A.*, 2007, **104**, 6908; (b) H. V. Huynh, L. R. Wong and P. S. Ng, *Organometallics*, 2008, **27**, 2231; (c) C. Taubmann, K. Ofele, E. Herdtweck, and W. A. Herrmann *Organometallics,* 2009, **28**, 4254; (d) Y. Zhang, J. C. Lewis, R. Bergman, J. A. Ellman and E. Oldfield, *Organometallics*, 2006, **25**, 3515; (e) W. Yao, O. Eisenstein and R. H. Crabtree, *Inorg. Chim. Acta*, 1997, **254,** 105; (f) J. Sabmannshausen, *Dalton Trans.*, 2012, **41**, 1919; (g) K. A. Siddiqui and E. R. T. Tiekink, *Chem. Commun.,* 2013, **49**, 8501 (h) S. Scholer, M. H. Wahl, N. I. C. Wurster, A. Puls, C. Hattigb and G. Dyker *Chem. Commun*.**,** 2014, **50**, 5909.

16 (a) M. Bousseau, L. Valade, J. P. Legros, P. Cassoux, M. Garboukas and L. V. Interrante, *J. Am. Chem. Soc.*, 1986, **108**, 1908; (b) P. Cassoux and L. Valade, *Inorganic Materials, John Wiley and Sons*, Chichester, 1996.

17. A. B. P. Lever, *Inorganic Electronic Spectroscopy*, *Elsevier*, *Amsterdam*, 1984.

18. E. R. T. Tiekink and J-Z. Schpector, *Chem. Comm*., 2011, **47**, 6623.

19. CrysAlis RED program, *Oxford Diffraction*, Abingdon, U.K. 2008.

20. G.M. Sheldrick, SHELXS97 and SHELXl97, Programs for Crystallographic Solution and Refinement, *Acta Crystallogr. Sect. A*, 2008, **64**, 112.

21. M. N. Burnett, C. K. Johnson, ORTEP-III, Oak Ridge Thermal Ellipsoid Plot Program for Crystal Structure Illustrations, Report ORNL-6895, *Oak Ridge National Laboratory*, Oak Ridge, TN, USA, 1996.

22. M. J. Frisch, G. W.Trucks, H. B. Schlegel, G. E. Scuseria, M. A. Robb, J. R. Cheeseman, J. A. Montgomery, T. Vreven, K. N. Kudin, J. C. Burant, J. M. Millam, S. S. Iyengar, J. Tomasi, V. Barone, B. Mennucci, M. Cossi, G. Scalmani, N. Rega, G. A. Petersson, H. Nakatsuji, M. Hada, M. Ehara, K. Toyota, R. Fukuda, J. Hasegawa, M. Ishida, T. Nakajima, Y. Honda, O. Kitao, H. Nakai, M. Klene, X. Li, J. E. Knox, H. P. Hratchian, J. B. Cross, V. Bakken, C. Adamo, J. Jaramillo, R. Gomperts, R. E. Stratmann, O. Yazyev, A. J. Austin, R. Cammi, C. Pomelli, J. W. Ochterski, P. Y. Ayala, K. Morokuma, G. A. Voth, P. Salvador, J. J. Dannenberg, V. G. Zakrzewski, S. Dapprich, A. D. Daniels, M. C. Strain, O. Farkas, D. K. Malick, A. D. Rabuck, K. Raghavachari, J. B. Foresman, J. V. Ortiz, Q. Cui, A. G. Baboul, S. Clifford, J. Cioslowski, B. B. Stefanov, G. Liu, A. Liashenko, P. Piskorz, I. Komaromi, R. L. Martin, D. J. Fox, T. Keith, M. A. Al-Laham, C. Y. Peng, A. Nanayakkara, M. Challacombe, P. M. W. Gill, B. Johnson, W. Chen, M. W. Wong, C. Gonzalez and J. A. Pople, *Gaussian 03*, revision C.02; Gaussian, Inc.: Wallingford . CT, U.S.A.

